Eksploatacja i Niezawodnosc – Maintenance and Reliability
Volume 23 (2021), Issue 4
journal homepage: http://www.ein.org.pl

Article citation info:
Vaičiūnas G, Steišūnas S, Bureika G. Specification of estimation of a passenger car ride smoothness under various exploitation conditions. Eksploatacja i Niezawodnosc – Maintenance and Reliability 2021; 23 (4): 719–725, http://doi.org/10.17531/ein.2021.4.14.

Specification of estimation of a passenger car ride smoothness under various exploitation conditions

Indexed by: Web of Science Group

Gediminas Vaičiūnas[a*], Stasys Steišūnas[a], Gintautas Bureika[a]

[a] Vilnius Gediminas Technical University, Faculty of Transport Engineering, Saulėtekio al. 11, LT-10223 Vilnius, Lithuania

Highlights

- Sperling's comfort index dependence on the stiffness of passenger car suspension.
- Wheel flat impact on rail vehicle running gear vibration character.
- Guidance & stability of running gear with independently rotating wheels.
- Processing of the carbody acceleration amplitudes by Fourier transform method.

Abstract

The stability and smoothness of rolling stock running could be defined accurately by universal Sperling's comfort index. The divergences of variation of Sperling's comfort index of a passenger car under specific operating conditions of running gear are examining in this paper. Numerical simulations of a passenger car running with independently rotating wheels under various conditions have been performing. Gained results showed that divergences of the Sperling's comfort index variation are particularly significant due to running gear component oscillations in the horizontal plane (lateral direction). A field experiment of a passenger car with a solid (traditional) wheelset with a flat running surface proved this hypothesis. The obtained results of this experiment confirmed this assumption. Therefore, the study of the regularities of lateral oscillations of a passenger car is the logical direction of further research.

Keywords

railway transport, passenger car, running gear, independently rotating wheels, Sperling's comfort index, divergences, numerical simulation, software package UM.

1. Introduction

The improvement of rolling stock raises several problems of the mechanical wheel-rail interaction: the risk of derailment, the intensity of rolling surface wear and the discomfort caused to passengers by vibrations [12, 14, 30]. In typical cases, technical solutions are under development to eliminate these problems. However, there are also unsolved aspects of the problems as mentioned above.

The wheel conicity ensures the stability and guidance of rolling stock with solid (ordinary) wheelsets and uniform rotational speed, respectively higher or lower linear speed in contact with rails [23]. It does not work on rail vehicles with independently rotating wheels, so other methods are needed. The damping of rolling contact of wheel and rail in dry friction provided by the primary suspension dampers of cargo rolling-stocks is considered in numerical simulations performed by Polish scientist Piotrowski [22]. Noticeable that the stability and smoothness of rolling stock running influenced the wear intensity of running gear and track components [11, 26].

The proposed power-steering railway bogie consists of independently rotating wheels (IRWs) with a power-steering device. It enables us to eliminate steering vibration while realising ideal steering with slight power assist on curving [3, 18]. There is a proposed use of IRWs with inverse tread conicity to get self-steering ability without any complex bogie structure. The testing and numerical simulation results show that the proposed IRWs with inverse tread conicity have good performance [27, 28]. The benefits of implementing active steering systems in railway vehicles mounting bogies with IRWs and outlines a design methodology for such systems are presented [21].

Noticeably that the parameters and characteristics of wheelsets with IRWs are regulated by law. In research, scientists also examine them, for example, the standard ISO 2631, EN 12299:2009 [10]. However, legal issues are not the subject of this research.

Solving rolling stock stability issues leads to passenger comfort issues, and peculiarities also occur here. One of them is passenger comfort in terms of vibrations. The Sperling's comfort index (SCI) is commonly used in scientific research to assess the passenger car ride smoothness in terms of vibrations. One of the main directions of railway development is to increase the running speed of trains. Naturally, research is usually carried out at high speeds, and the SCI is examined at high speeds (more than 160 km/h). However, with the development of rail transport, specific cases always occur, such as running vehicles with IRWs on small radius curves (less than 300 m radii). This refers to railway track repair works, where vehicles need to move from one track to another or manoeuvring in railway stations or tunnels. In this case, the speed is lower (there may be restrictions of 50 km/h and less). Passenger car ride smoothness is also essential here, and a study of the SCI for such issues is needed. The rolling surface of the wheels could be damaged when vehicles are running on poor quality railway tracks. With larger than the allowable damage, continued running on

(*) Corresponding author.
E-mail addresses: G. Vaičiūnas - gediminas.vaiciunas@vilniustech.lt, S. Steišūnas - stasys.steisunas@vilniustech.lt, G. Bureika - gintautas.bureika@vgtu.lt

rail vehicles is prohibited. However, the permissible extent of damage caused by vibrations affects passenger car ride smoothness and must be estimated by SCI.

Examples of the study of the impact of rolling stock wheels with damage on the rails and on the rail vehicle ride smoothness are described in scientific papers [2, 20]. The most common damage to the wheelset is the unevenness of the rolling surface, the wear of the flange, wheel flats and cracks. The unevenness of the wheel rolling surface of the wheels can be divided into three types according to their effect on the rail:

1. Unevenness causing impact and loss of contact (flats, bends, abrasions, cracks, etc.). The unevenness of the wheel rolling surface is usually characterised by the depth and the length of the flat.
2. Insulated irregularities increase the vertical impact of the wheel on the rail without loss of contact (uneven wear, "out-of-roundness", etc.).
3. Wheel flange damage. The flange prevents the wheelset from the derailment. A wheel is considered unusable and unsafe when its flange is critically thinned (equal to or less than 25 mm).

Problematic of wheel rolling surface are considered in the most publications about the long-term interaction between rolling stock running gear and track [8, 17, 4], the intensity of wheelset wear is also examined [1, 7, 13, 23]. The phenomena of wheelset wear have been extensively studied [1, 6, 15]. The wear of the wheel rolling surface is divided into even and uneven. Even wear is wear of the wheel rolling surface when the wheel rolling surface wears evenly (regular "circle"). Uneven wear of the wheel rolling surface differs from even wear in that the rolling surface wears unevenly ("out-of-roundness"), which increases the dynamic impact of the wheel on the rail [15, 25]. It is difficult to find such damage without removing the wheelset during a wagon inspection, as uneven wear can account for one-fifth or more of the total wheel surface [28].

The flats are the most common wheel running surface damages due to wheelset slip or jammed brake pads [5, 27, 31]. Flats result from wheel skidding, wheel jamming, or brake failure (especially during the wagon sorting on hubs). Flats occur in winter much more often than in summer. Mathematical models of the impact effect of wheelset with a flat on the rail have been discussed in the works of various scientists [5, 26].

The combination of short-term dynamics and long-term wear processes is a very complicated and unexplored phenomenon, but the influence of physical factors such as surface unevenness, material properties, or micro-crack intensity must be considered [24, 32]. In most scientific research, wear processes are usually simplified and conditioned only by frictional forces, and the dependence on plastic deformation and other processes influencing the formation of cracks are not considered [20, 16]. The study of wheelset damage observed that the damage formation process is a complicated and complex process. Finally, the analysis of wheelset damage shows that the safe and smooth movement of rolling stock is greatly influenced by the shape and condition of the rolling surface of the wheelset wheel [9].

Some research has been performed by scientists of Korea Railroad Institute to correlate various evaluation methods by using different vibration models [12]. The ride comfort indexes defined in ISO 2631 and EN 12299:2009 are commonly adopted in favour of the SCI method is seldom applied and discussed. Ride comfort in railway vehicles on a track with vertical irregularities was evaluated by implementing two different comfort indexes, corresponding to the EN 12299:2009 and SCI method, respectively [24]. The ride comfort level of passengers in two positions, sitting and standing, was compared using the EN 12299:2009 and SCI methods [19]. The Ride Comfort Index discussed in both studies is the Mean Comfort Index. Another frequently used Ride Comfort Index in EN 12299:2009 is called the Continuous Comfort Index. This index uses a quadratic average (r.m.s) of the frequency weighted accelerations measured to evaluate the Mean Comfort [14]. Since the mean comfort is determined in the longitudinal, lateral, and vertical directions, respectively, and it has similarities to Sperling's comfort index.

Based on a comparative analysis of the methods in the literature, the SCI was selected by Authors as the most appropriate indicator to assess the running comfort of a passenger car. This study aims to provide different ways of SCI identification under specific operating conditions of passenger wagon, such as running on a small radius curve of a track or when the wheel running surface is damaged. In order to reduce the intensity of wear of the rolling stock wheel flange due to the friction on the track curves, the possibility of installing IRWs on the rolling stock (instead of the usual solid wheelsets) is investigated. Various issues of rail vehicle running smoothness are examined in the research, as one of the main subjects is rail vehicles' stability.

2. Methodology of research on running gear vibration

During the assessment of rail vehicle running gear vibration level and considering the passenger comfort, the SCI was used as an indicator of running smoothness [6, 29]. The value of SCI was calculated according to the formula:

$$W_Z = \left(\sum_{i=1}^{n_f} W_{Z_i}^{10} \right)^{\frac{1}{10}}, W_{z_i} = \left[a_i^2 B(f_i)^2 \right]^{\frac{1}{6.67}}, \tag{1}$$

where: n_f - the number of frequencies considered, a – carbody acceleration, m/s^2, f_i – vibration frequency, Hz, $B(f_i)$ – frequency and vibration direction coefficient influencing the passenger well-being:

$$B(f_i) = k\sqrt{\frac{1.911 f_i^2 + (0.25 f_i^2)^2}{(1 - 0.277 f_i^2)^2 + (1.563 f_i - 0.0368 f_i^3)^2}}, \tag{2}$$

where: k = 0.737, if oscillations are lateral, and k = 0.588 if oscillations are vertical.

The smooth-running indicators calculated based on Equations (1-2) are compared with the standard assessment scale. The quality of rail vehicle running gear behaviour is finally assessed according to comparative results.

At SCI values up to 1, the human senses do not feel the impact of vibrations; at SCI values from 1 to 3, vibrations are felt but do not cause any discomfort, and at SCI values from 3.0 to 3.5, the discomfort is felt. Exceeding the SCI value of more than 4, the vibrations are hazardous to human health. Therefore, the SCI limit for vehicles is taken up to 3.25.

Based on this methodology, examples of the values of the SCI under the specific operating conditions of a passenger car running gear are further analysed, for example, the case of a passenger car with independently rotating wheels, a small radius curve or when the wheel running surface has damage.

At first, the SCI was modelled for a passenger car with IRWs and with typical (unmodified) suspension, which parameters are presented in Table 1.

Table 1. Typical parameters for passenger car suspension

Parameter	Value
Primary suspension stiffness coefficient in the lateral direction, N/m	$1 \cdot 10^6$
Primary suspension stiffness coefficient in the vertical direction, N/m	$1 \cdot 10^6$
Secondary suspension stiffness coefficient in the lateral direction, N/m	$2 \cdot 10^5$
Secondary suspension stiffness coefficient in the vertical direction, N/m	$2 \cdot 10^5$
Total damping factor of primary and secondary suspension, Ns/m	$1 \cdot 10^4$

3. Results of numerical modelling of a passenger car running

3.1. Sperling's comfort index values of typical suspension of passenger car

During the study, SCI in lateral and vertical directions at different running speeds were simulated by software package "Universal Mechanism" (UM) on different sections of the track. The obtained values of SCI are provided in Figure 1 and Figure 2.

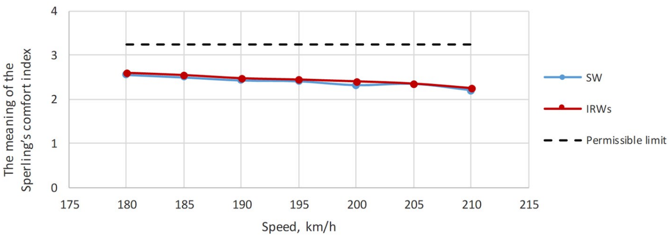

Fig. 1. Sperling's comfort index values in the vertical direction in the track tangent section

The diagram of Figure 1 shows that the SCI (in terms of vertical oscillations) decreases steadily with increasing speed from 180 km/h for both the one solid wheelset (SW) and the independently rotating wheels.

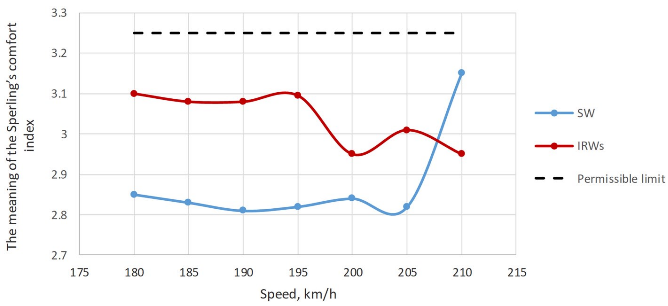

Fig. 2. Sperling's comfort index values in the lateral direction in the track tangent section

The curves of Figure 2 show that divergences occur in the variation of the SCI in terms of lateral vibrations at a speed of 200 km/h. Examining the change of the SCI according to the speed when the track section is tangent, different tendencies of the criterion change can be seen by analysing the oscillations in the vertical and horizontal planes. The values calculated from the vibration parameters of the vertical plane decrease gradually with increasing speed from 180 km/h to 210 km/h. Meanwhile, in the horizontal plane, at a speed of 200-210 km/h, divergences of value change are observed. The graphs of the variation of the values of the SCI in the 200 m radius curve according to the speed are shown in Figure 3 and Figure 4.

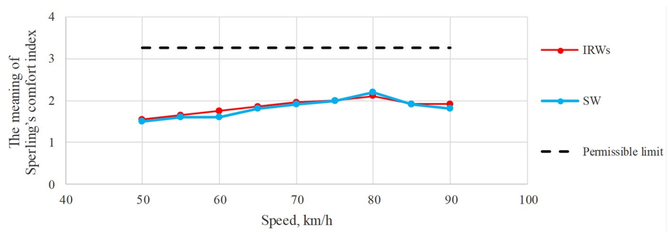

Fig. 3. Sperling's comfort index values in the vertical direction in 200 m radius curve

The diagram of Fig. 3 shows that the SCI changes consistently in terms of vertical oscillations, and in the 200 m radius curve, only the lower speed range is considered in the curve; the SCI, in this case, increases consistently (almost consistently).

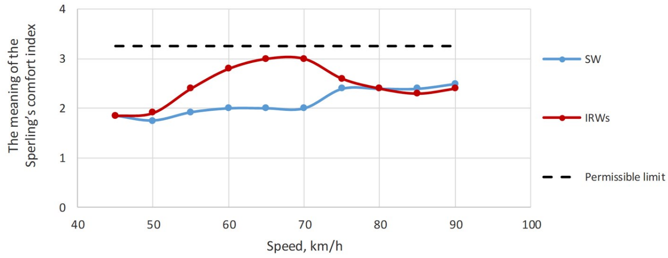

Fig. 4. Sperling's comfort index values in the lateral direction in 200 m radius curve

As in the tangent section of the track, divergences (in the speed range 60-70 km/h) are observed in the change of the SCI in terms of lateral oscillations with the 200 m radius curve (Fig. 4). Examining the change of the SCI in terms of the speed at the 200 m radius of the track curve, as in the case of a tangent track, different trends of the criterion change can be seen by analysing the oscillations in the vertical and lateral planes. The values calculated from the vertical plane oscillation parameters increase steadily as the speed increases from 50 km/h to 80 km/h (the trend changes slightly at 90 km/h). In the horizontal plane, at speeds of 60-70 km/h, the divergences of change of SCI values are observed. The Authors of the study pointed out that so far, only cases with standard passenger car suspension have been considered. By changing the stiffness of the rail vehicle suspension, the dynamic parameters of the passenger car running also change.

3.2. Sperling's comfort index values of adjusted suspension of passenger car

In order to improve the dynamic parameters of the passenger car with IRWs, the stiffness values of the primary and secondary suspension elements of their running gear were adjusted. Prior to adjusting the values, a study was performed to determine how the mean square of carbody accelerations depend on the stiffness of the respective suspension [28]. The dependences of the mean square of carbody accelerations on the stiffness of the primary suspension are presented in Figure 5 and Figure 6.

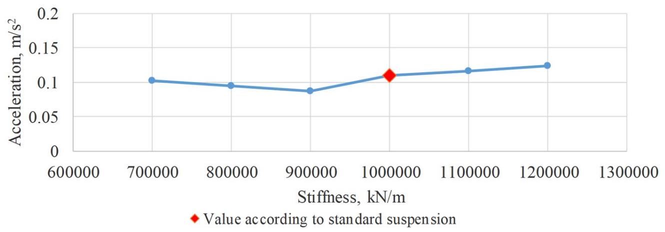

Fig. 5. Dependence of mean square of carbody accelerations on the vertical stiffness of the primary suspension

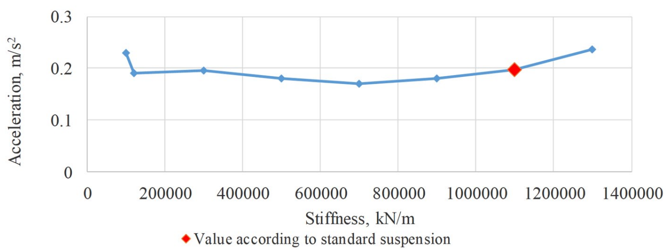

Fig. 6. Dependence of mean square of carbody accelerations on the lateral stiffness of the primary suspension

The dependences of the mean square of carbody accelerations on the vertical and the lateral stiffness of the primary suspension, respectively, indicate that the stiffness of the standard suspension elements needs to be adjusted to improve the dynamic characteristics of the passenger car with IRWs.

The dependences of the mean square of carbody accelerations on the stiffness of the secondary suspension are presented in Figure 7 and Figure 8.

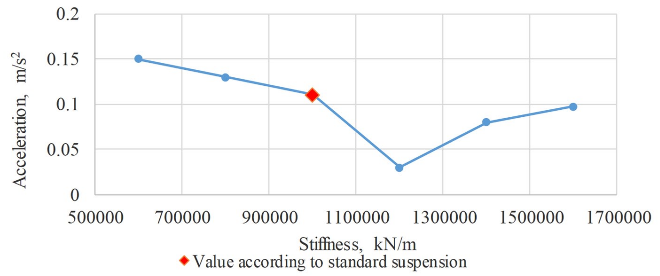

Fig. 7. Dependence of mean square of carbody accelerations on the vertical stiffness of the secondary suspension

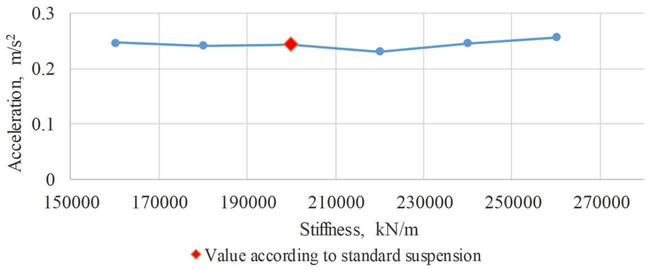

Fig. 8. Dependence of mean square of carbody accelerations on the lateral stiffness of the secondary suspensionsuspension

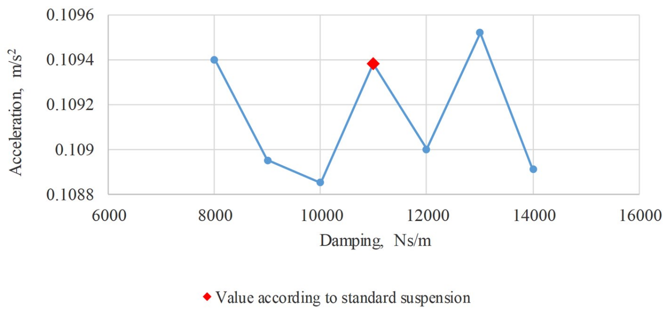

Fig. 9. Dependence of mean square body accelerations on secondary suspension damping parameters

The dependence of the mean square of carbody accelerations on the secondary suspension damping parameters is shown in Figure 9.

The dependence of the mean square of carbody accelerations of the secondary suspension for vertical and lateral stiffness, respectively, as well the dependence on the mean square carbody accelerations on the secondary suspension damping parameters indicate that the stiffness of the standard suspension elements also needs to be adjusted to improve the IRW dynamic performance.

Based on the research data, the stiffness values of the suspension elements were chosen. These data are submitted in Table 2.

By using the newly selected values of the stiffness of the passenger car suspension elements, the regularities of the change of SCI values were remodelled. SCI gained values are presented in Figures 10 and Figure 11, respectively.

The curves of Fig. 10 show that in the case of a standard suspension, the SCI on tangent track (in terms of vertical vibrations) decreases steadily with increasing the speed from 180 km/h for both the SW and the IRWs.

The curves of Figure 11 show that, as with the standard suspension, the SCI divergences occur on the tangent section in the variation of the SCI in terms of lateral vibrations. This is especially true in the case

Table 2. Values of stiffness coefficients of passenger car suspension elements after adjustment

Parameter	Value
Primary suspension stiffness coefficient in the lateral direction, N/m	$9{\cdot}10^5$
Primary suspension stiffness coefficient in the vertical direction, N/m	$9{\cdot}10^5$
Secondary suspension stiffness coefficient in the lateral direction, N/m	$2.2{\cdot}10^5$
Secondary suspension stiffness coefficient in the vertical direction, N/m	$1.2{\cdot}10^6$
Total damping factor of primary and secondary suspension, Ns/m	$7{\cdot}10^4$

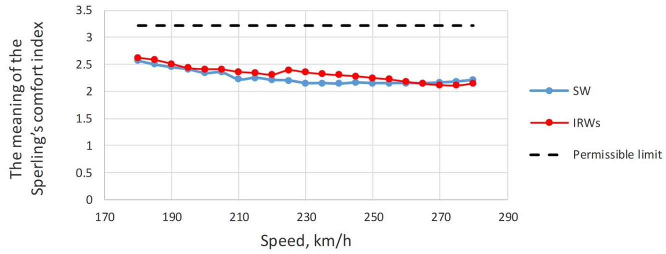

Fig. 10. The value of the Sperling's comfort index in the vertical direction in tangent track

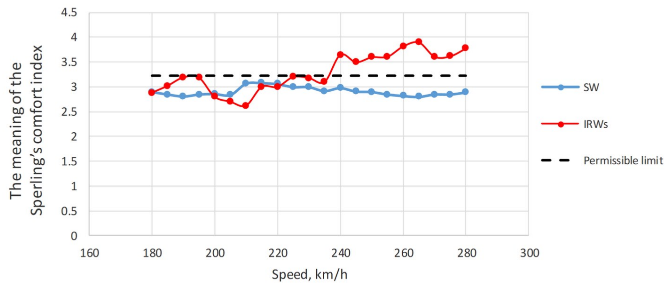

Fig. 11. The value of the Sperling's comfort index in the lateral direction in tangent track

of IRWs. Comparing the tendencies of the change of the value of the SCI on the track tangent section in the vertical and lateral directions was noticed that in the vertical direction, the consistent decrease is observed with increasing running speed. The divergences of change of SCI value in the lateral direction in the, are observed when the speed of a passenger car with IRWs reaches the values of (240-280) km/h.

The variation of SCI values on the 200 m radius curve is shown in Figure 12 and Figure 13.

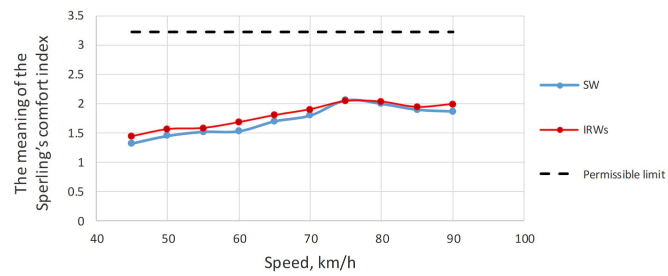

Fig. 12. The value of the Sperling's comfort index in the vertical direction in a 200 m radius curve

SCI values in the vertical direction on a track curve with a radius of 200 m, as in the case of a standard suspension, changes consistently, i.e. without observable divergences.

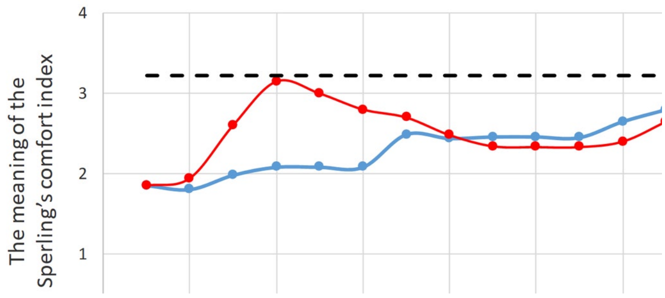

Fig. 13. The value of the Sperling's comfort index in the lateral direction on a curve with a radius of 200 m

The divergences of the variation of SCI values in the lateral direction on the 200 m radius curve of the track, as in the case of standard suspension, were observed. The change of SCI values according to the speed in the 200 m radius curve shows the same tendencies as previously analysed: in the lateral direction – consistent change, in the lateral direction – divergences appear.

The modelling results show that the divergences of the change of the SCI occur precisely due to the oscillations in the lateral direction. This fact raises the question to the study Authors as to whether this is not a systematic error in the modelling (e.g., the assumption made in the programmed conditions). For searching for an answer to this question, the Authors of this study conducted further study, which included not only the theoretical calculation of the SCI but also its determination based on the vibration parameters measured in field tests. A specific case of observation was a passenger car with a damaged wheel.

3.3. Sperling's comfort index values in case of a damaged wheel

As in the other cases examined, the SCI in the presence of a damaged wheel was primarily modelled by numerical simulation. These wheel damage parameters for the modelling were selected: flat depth $h = 0.001$ m and length $L = 20$ mm.

After having processed the data obtained during the simulation by means of the Fourier transform method, the dependence of the vehicle body acceleration amplitude repetitions on the running time was obtained. These data make it possible to assess the comfort of the passengers through the SCI. The obtained SCI values are shown in Figure 14.

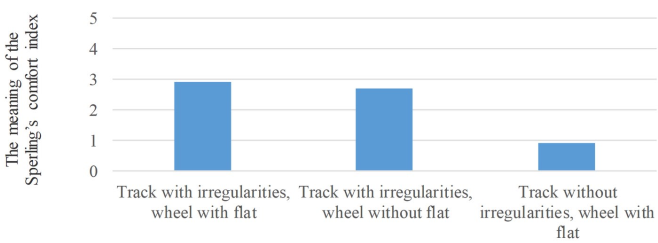

Fig. 14. Values of Sperling's comfort index

The diagram of Figure 14 shows that the SCI values of running smoothness are acceptable (see Table 2) when the passenger cars operate with the damaged wheel with a flat depth of 1 mm depth and a length of 20 mm on the track tangent section. However, after introducing track roughness, the SCI values increased about 3 times and approached the limit values for passenger cars.

To test these data and the previously hypothesised that the divergences of the change of the SCI values occur when examining the oscillations in the lateral direction of the passenger car, a field test (experiment) was performed. During it, the oscillations of the passenger carbody were measured in practice, and the trends of SCI value change were determined based on the results.

4. Identification of passenger car running smoothness parameters by field testing

The main parameters of the measurement equipment used for the experiment are presented in Table 3. The mounting of the sensors in the passenger car is shown in Figure 15. The recorded data of the experiment were estimated by the SCI for the assessment of smoothness of passenger car rides, and gained results are presented in Figure 16.

As seen from Figure 16, the SCI values comply with the requirements for ride stability, sufficient for passenger cars, whereas good results have not been reached in the lateral direction. The highest value of the index in lateral direction has been reached at the running speed of 40 km/h, while with speed increasing, the index values went on decreasing. The SCI values received in the vertical direction fluctuates in the zone of "sufficient for passenger cars". With the car running speed augmenting, they are evenly increasing.

Table 3. Basic parameters of the equipment used for the experiment

Equipment	Measurement limits, g	Measurement frequency, Hz	Sensor mass, kg	Accuracy, %
Corrsys-Datron HF-500C	±3	10	0.230	±0.2
Kistler Type 8395A	±3	1000	0.155	±0.2

Fig. 15. Mounting of the sensors in the passenger car

The insight of the experiment is that SCI values in terms of vertical oscillations change consistently with varying speeds. In contrast, the regularity of the change of these values in the lateral direction deviates from the consistent change. Therefore, it is expedient to analyse the regularity of the change of the values of the SCI according to the vibrations in the lateral direction.

The experimentally determined regularity of the change of the SCI (according to the oscillations in the lateral direction) can be described by the equation of the 2nd, the 3rd or the 4th degree, respectively, the following expressions are possible:

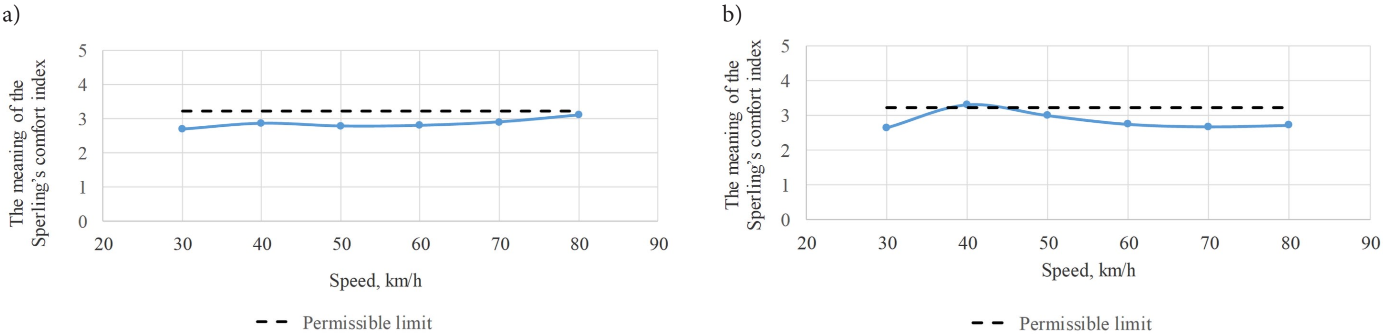

Fig. 16. Experimental Sperling's comfort index values at different running speeds: a) in vertical direction; b) in lateral direction

$$f(x) = p_1x^2 + p_2x + p_3;$$
$$f(x) = p_1x^3 + p_2x^2 + p_3x + p_4; \quad (3)$$
$$f(x) = p_1x^4 + p_2x^3 + p_3x^2 + p_4x + p_5.$$

The values of the coefficients pi of the 2nd, the 3rd and the 4th-degree function (coefficients 3, 4 and 5, respectively) and the coefficients of determination R^2, respectively, are given in Table 4.

Table 4. Coefficients of polynomial function according to experimental data

Coefficients	Values		
	The 2nd degree function	The 3rd degree function	The 4th degree function
p_1	– 0.0004	0.00005	– 0.000002
p_2	0.0369	– 0.0092	0.0006
p_3	2.0884	0.494	– 0.0492
p_4	-	– 5.304	1.848
p_5	-	-	– 21.69
R^2	0.304	0.8628	0.9938

According to the last row of Table 4, the coefficient of determination of the 2nd-degree mathematical correlation is too small: R^2 = 0.304, the coefficient of determination of the 3rd-degree function R^2 = 0.8628, and the coefficient of determination of the 4th-degree function R^2 = 0.9938 – very strong mathematical correlation. It can be concluded that it is recommended to describe the regularity of the variation of SCI according to the rail vehicle speed with the equation (polynomial) of the 3rd or the 4th degree. The accuracy of SCI description ensures the possibility to maintain an acceptable level of a passenger car running smoothness during exploitation.

5. Conclusions

The investigation of the tendency of Sperling's comfort index variation is an appropriate way to define the smoothness of passenger cars under various exploitation conditions. By monitoring the variation of the Sperling's comfort index according to the running speed of the vehicle, ride smoothness level can be assessed. In cases such as when vehicle running gear is with independently rotating wheels, when a car is curving the small radius curves of a track or when the wheel surfaces are damaged.

To verify the suitability of Sperling's comfort index for assessing the smoothness of a passenger car ride, the Authors performed a numerical simulation of the vehicle with independently rotating wheels. These simulations are running in a track tangent section and 200 m radius track curve and adjusting the passenger car suspension parameters.

The Authors also performed a numerical simulation and experimental research of a passenger car with a damaged wheel running surface and compared the obtained results. During examining the variation of the Sperling's comfort index according to the running speed of the vehicle, it was observed that to operate the vehicles safely with independently rotating wheels, and it is necessary to adjust the suspension parameters of the passenger car. It is necessary to change the stiffness and damping of the primary and secondary suspension parameters. Otherwise, Sperling's comfort index values, especially in the lateral direction, change chaotically and indicate the inadmissible quality of ride smoothness control.

After summarising the results of this study, the Authors recommend describing the tendency of the variation of the Sperling's comfort index (considering the running gear oscillations in the lateral direction) according to the rail vehicle speed, with the equations of the 3rd or the 4th-degree. The coefficient of determination was defined by describing the dependence of the 4th-degree function (R^2=0.9938 – a very strong mathematical correlation).

The investigation of vibration parameters of passenger cars shows that the divergences of the change of the Sperling's comfort index occur especially due to the oscillations in the lateral direction – this is confirmed both by theoretical calculations and by vibration parameters measured in practice. Therefore, the study of the regularities of lateral oscillations of a passenger car is a reasonable direction for further research.

Acknowledgment

The research is funded by the EU Shift2Rail project GEARBODIES (Grand number: 10101396) under Horizon 2020/ Shift2Rail Framework Programme.

References

1. Brommundt E. A simple mechanism for the polygonalization of railway wheels by wear. Mechanics Research Communications and Applied 1997; 24(2): 435-442, https://doi.org/10.1016/S0093-6413(97)00047-5.
2. Bureika G, Levinzon M, Dailydka S, Steišūnas S, Žygienė R. Evaluation criteria of wheel/rail interaction measurement results by trackside control equipment. International Journal of Heavy Vehicle Systems 2019; 26(6): 747-764, https://doi.org/10.1504/IJHVS.2019.102682.
3. Dukalski P, Będkowski B, Parczewski K, Wnęk H, Urba ś A, Augustynek K. Dynamics of the vehicle rear suspension system with electric motors mounted in wheels. Eksploatacja i Niezawodnosc - Maintenance and Reliability 2019; 21(1): 125-136, https://doi.org/10.17531/ein.2019.1.14.
4. Ekberg A, Kabo E. Fatigue of railway wheels and rails under rolling contact and thermal loading-an overview. Wear 2005; 258(8): 1288-1300, https://doi.org/10.1016/j.wear.2004.03.039.

5. Favorskaya A, Khokhlov N. Modelling the impact of wheelsets with flat spots on a railway track. Procedia Computer Science 2018; 126: 1100-1109, https://doi.org/10.1016/j.procs.2018.08.047.
6. Frischmuth K, Langemann D. Numerical Analysis of long-term wear models. Machine Dynamics Problems 1998; 20: 113-122.
7. Grassie S, Gregory R, Harrison D, Johnson K. The dynamic response of railway track to high frequency vertical, lateral, longitudinal excitation. Journal of Mechanical Engineering Science 1982; 24(2): 77-102, https://doi.org/10.1243/JMES_JOUR_1982_024_016_02.
8. Gorbunov M. Kravchenko K. Bureika G. Gerlici J. Nozhenko O. Vaičiūnas G. Bučinskas V, Steišūnas S. Estimation of sand electrification influence on locomotive wheel/ rail adhesion processes. Eksploatacja i Niezawodnosc - Maintenance and Reliability 2019; 21(3): 460-467, https://doi.org/10.17531/ein.2019.3.12.
9. Hayes W, Tucker H. Wheelset-track resonance as a possible source of corrugation wear. Wear 1991; 144(1-2): 211-226, https://doi.org/10.1016/0043-1648(91)90016-N.
10. Jiang Y, Bernard K, Chen B. K, Thompson C. A comparison study of ride comfort indices between Sperling's method and EN12299. International Journal of Rail Transportation 2019; 7(4): 1-18, https://doi.org/10.1080/23248378.2019.1616329.
11. Jin X, Xiao X, Wen Z, Guo J, Zhu M. An investigation into the effect of train curving on wear and contact stresses of wheel and rail. Tribology international 2009; 42(3): 475-490, https://doi.org/10.1016/j.triboint.2008.08.004.
12. Kim Y, Kwon H, Kim S. Correlation of ride comfort evaluation methods for railway vehicles. International Journal of Rail Transportation 2003; 17(217): 73-88, https://doi.org/10.1243/095440903765762823.
13. Kowalski S. The influence of selected PVd coatings on fretting wear in a clamped joint based on the example of a rail vehicle wheel set. Eksploatacja i Niezawodnosc - Maintenance and Reliability 2018; 20(1): 1-8, https://doi.org/10.17531/ein.2018.1.1.
14. Kufver B, Persson R, Wingren J. Certain aspects of the CEN standard for the evaluation of ride comfort for rail passengers. WIT Transactions on The Built Environment 2010; 29: 605-614, https://doi.org/10.2495/CR100561.
15. Kusel M, Brommundt E. The evolution of noncircularities at braked or driven railway wheels. Machine Dynamics Problems 1998; 20: 313-324.
16. Ma Ch, Gao L, Xin T, Cai X, Nadakatti M, Wang P. The dynamic resonance under multiple flexible wheelset-rail interactions and its influence on rail corrugation for high-speed railway. Journal of Sound and Vibration 2021; 498, https://doi.org/10.1016/j.jsv.2021.115968.
17. Meywerk M. Polygonalization of railway wheels. Archive of Applied Mechanics 1999; 69(2): 105-120, https://doi.org/10.1007/s004190050208.
18. Michitsuji Y, Suda Y. Running performance of power-steering railway bogie with independently rotating wheels. Vehicle System Dynamics 2006; 4(1): 71-82, https://doi.org/10.1080/00423110600867416.
19. Munawir T, Samah A, Rosle M. A comparison study on the assessment of ride comfort for LRT passengers. International Research and Innovation Summit (IRIS2017), 2017, https://doi.org/10.1088/1757-899X/226/1/012039.
20. Peng B, Iwnicki S, Shackleton Ph, Crosbee D, Zhao Y. The influence of wheelset flexibility on polygonal wear of locomotive wheels. Wear 2019; 432-433, https://doi.org/10.1016/j.wear.2019.05.032.
21. Perez J, Mauer M, Busturia J. M. Design of Active Steering Systems for Bogie-Based Railway Vehicles with Independently Rotating Wheels. Vehicle System Dynamics 2002; 37(1): 209-220, https://doi.org/10.1080/00423114.2002.11666233.
22. Piotrowski J. A substitute model of two-dimensional dry friction exposed to dither generated by rolling contact of wheel and rail. Vehicle System Dynamics 201; 50(10): 1495-1514, https://doi.org/10.1080/00423114.2012.676653.
23. Polach O. Wheel profile design for the target conicity and wide tread wear spreading. Wear 2011; 271(1-2): 195-202, https://doi.org/10.1016/j.wear.2010.10.055.
24. Popp K, Kruse H, Kaiser I. Vehicle-track dynamics in the mid-frequency range. Vehicle system dynamics C. International Journal of Vehicle Mechanics and Mobility 1999; 31(5-6): 423-464, https://doi.org/10.1076/vesd.31.5.423.8363.
25. Pradhan S, Samantaray A, Bhattarcharyya R. Evaluation of ride comfort in a railway passenger vehicle with integrated vehicle and human body bond graph model. International Mechanical Engineering Congress and Exposition, 2017, https://doi.org/10.1115/IMECE2017-71288.
26. Sladkowski A, Pogorelov D. Investigation of the dynamic interaction in the wheel-rail contact in the presence of flat spots on the wheelset. Bulletin of the East Ukrainian National University 2008; 5(123): 88-95.
27. Suda Y, Wang W, Nishina M, Lin S, Michitsuji Y. Self-steering ability of the proposed new concept of independently rotating wheels using inverse tread conicity. Vehicle System Dynamics 2012; 50(1): 291-302, https://doi.org/10.1080/00423114.2012.672749.
28. Taletavičius, R. Rolling stock driving stability study. Master thesis, VGTU, 2019: 73.
29. Vaičiūnas G, Steišūnas S. Sperling's comfort index study in a passenger car with independently rotating wheels. Transport Problems 2021, 16(2): 121-130.
30. Vaičiūnas G, Bureika G, Steišūnas S. Research on metal fatigue of rail vehicle wheel considering the wear intensity of rolling surface. Eksploatacja i Niezawodnosc - Maintenance and Reliability 2018, 20(1): 24-29, https://doi.org/10.17531/ein.2018.1.4.
31. Wallentin M, Bjarnehed H, Lundén R. Cracks around railway wheel flats exposed to rolling contact loads and residual stresses. Wear 2005; 258(7-8): 1319-1329, https://doi.org/10.1016/j.wear.2004.03.041.
32. Ye Y, Sun Y, Shi D, Peng B, Hecht M. A wheel wear prediction model of non-Hertzian wheel-rail contact considering wheelset yaw: Comparison between simulated and field test results. Wear 2021; 474-475, https://doi.org/10.1016/j.wear.2021.203715.